

ORIGINAL RESEARCH ARTICLE

Nanosensor of gallium nitride for methanol adsorption for producing hydrogen: A computational chemistry study

Fatemeh Mollaamin^{1,2,*}, Majid Monajjemi³

¹ Department of Food Engineering, Faculty of Engineering and Architecture, Kastamonu University, Kastamonu 37100, Turkey

² Department of Biology, Faculty of Science, Kastamonu University, Kastamonu 37100, Turkey

³ Department of Chemical Engineering, Central Tehran Branch, Islamic Azad University, Tehran 1477893855, Iran

* Corresponding author: Fatemeh Mollaamin, smollaamin@gmail.com

ABSTRACT

The selective hydrogen production from methanol on the graphitic-like gallium nitride (GaN) and carbon doped gallium nitride (C-GaN) nanosheets has been challenged using the density functional theory (DFT) method. In this work, we report that GaN and C-doped GaN can catalyze the direct producing hydrogen (H₂) of methanol (CH₃OH) through Langmuir adsorption. The changes of charge density have shown a more important charge transfer for C-doped GaN compared to GaN which act both as the electron acceptor while CH₃OH molecules in water act as the stronger electron donors through adsorption on the GaN and C-doped GaN surfaces. The adsorption of CH₃OH molecules on the GaN and C-doped GaN surfaces represented spin polarization in the GaN and C-doped GaN which can be employed as three magnetic sensors for running the reaction of H₂ producing. The partial electron density states based on “PDOS” graphs have explained that the CH₃OH states in both of GaN and C-doped GaN nanosheets, respectively, have more conduction bands between -5 eV to -10 eV. The simulated distribution functions of CH₃O@GaN and CH₃O@C-GaN complexes exhibits that the bond lengths of O-Ga in CH₃O-GaN complex is 1.99 Å and O-C in CH₃O-C-GaN complex is 1.43 Å. Besides, the plot for electric potential versus atomic charge has been shown around carbon doping of the GaN which presents the electron accepting characteristics of this element via the electron donor of oxygen atom of hydroxyl group in CH₃OH with linear relation coefficient of $R^2 = 0.9948$. GaN and C-GaN nanosheets seem to have enough efficiency for adsorption CH₃OH molecules through charge transfer from oxygen to the gallium and carbon elements due to intra-atomic and interatomic interactions.

Keywords: CH₃O@GaN; CH₃O@C-GaN; H₂; DFT; Langmuir adsorption

ARTICLE INFO

Received: 2 June 2023
Accepted: 14 July 2023
Available online: 22 September 2023

COPYRIGHT

Copyright © 2023 by author(s).
Applied Chemical Engineering is published by EnPress Publisher, LLC. This work is licensed under the Creative Commons Attribution-NonCommercial 4.0 International License (CC BY-NC 4.0).
<https://creativecommons.org/licenses/by-nc/4.0/>

1. Introduction

Gallium nitride (GaN) structure is one of the most discovered group III-nitride semiconductors which have been applied in different applications like electronic, optoelectronic devices, and sensor instruments^[1-4]. Considering the prominent electronic properties of gallium nitride (GaN), it can be an appropriate case for gas sensing^[5-11]. For instance, some studies have exhibited that Ga₁₂N₁₂ nanoclusters are capable for gas sensing of CO, NO, NO₂, and HCN molecules^[12,13]. Moreover, GaN nanostructures suggest firm action under different radiation and in space conditions at room-temperature with wide varieties of temperature and humidity as compared to metal-oxides^[14]. In addition, it has been investigated that considering the interaction between gas molecule and surface in the active compound, the PL-GaN sheet could be applied as a largely selective magnetic gas detector for

nitric oxide (NO) and nitrogen dioxide (NO₂) sensing^[15,16]. Density functional theory (DFT) computations have accomplished and indicated that GaN wurtzoids as an agent of GaN nanocrystals are appropriate for hydrogen detecting nanostructures. One-dimensional semiconductor nanowires often consist of polytypic structures, due to the coexistence of various crystal GaAs as the semiconductors by using the chemical vapor transport approach^[17]. Concerning damaging impact of NO₂ on human health and environment makes NO₂ gas sensors and their state-of-the-art characteristics have been studied^[18–20]. Ammonia “NH₃” which is an important ingredient of reactive nitrogen, participates in prevalent harmful impacts on health. Nitrogen atom in NH₃ helps to form the atmospheric aerosols which remain in the atmosphere for some days^[21–23].

Recently, the ability of gallium nitride surface for the hydrogenation of carbon monoxide and carbon dioxide to dimethyl ether and their products have been evaluated using experimental and theoretical studies which introduce a different potent catalyst for direct hydrogenation of carbon dioxide to dimethyl ether^[24–26].

Therefore, this research wants to investigate the adsorption of CH₃OH and H₂O molecules on the monolayer graphitic GaN and C-doped GaN nanosheets with an atomically flat planar honeycomb hexagonal structure as “PL-GaN” employing density functional theory (DFT) towards the formation of H₂ and CO₂ products^[27–29].

2. Theoretical insights, applied material and method

In this research, the simulated calculations have been directed in the GaussView 6.06.16^[30] and calculated by Gaussian 16, Revision C.01^[31] using the DFT method. The [Perdew–Burke–Ernzerhof] “PBE” functional with high-precision generalized gradient approximation “GGA” has been employed to achieve more authentic results^[32]. Every simulated group contains a graphitic-like of length 25 Å with bond length of 1.95 Å for Ga–N in gallium nitride surface and bond length of 1.94 Å for C–N in carbon doped gallium nitride surface with a single CH₃OH and H₂O molecules adsorbed onto it (**Figure1**).

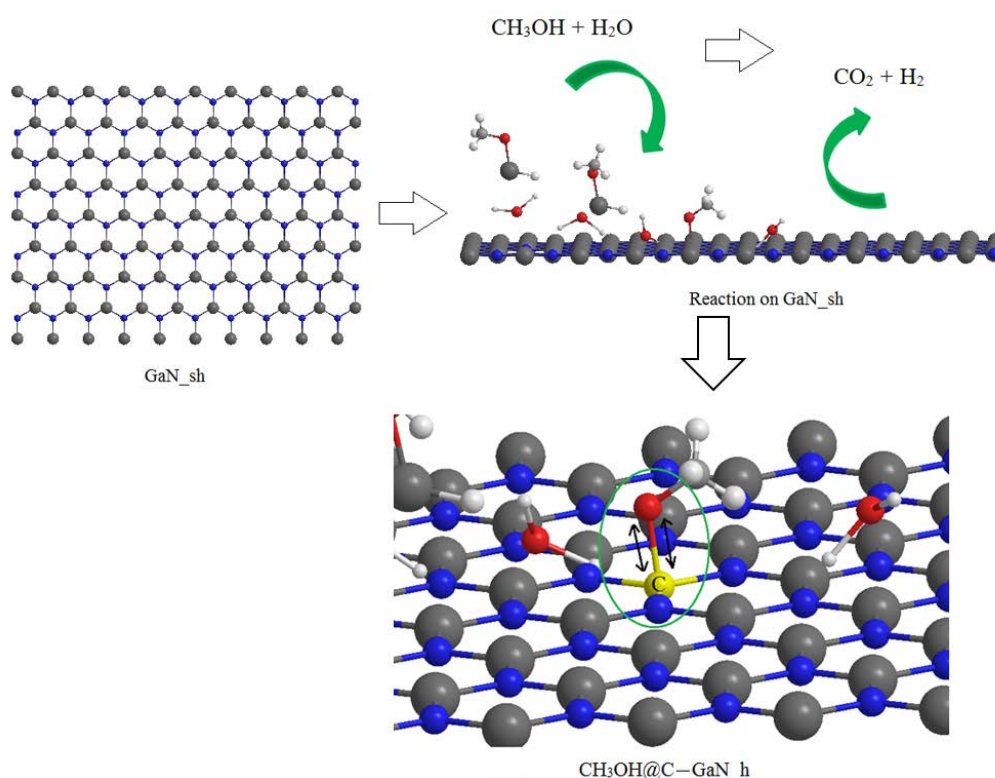


Figure 1. “Langmuir” adsorption of CH₃OH and H₂O molecules onto GaN and C–GaN nanosheets.

The charge transfer between adsorbates of CH₃OH and H₂O molecules and adsorbents of GaN and C-doped

GaN nanosheets is calculated due to the Bader charge analysis^[33]. This method can measure charge accumulation from the charge of each atom in the complex model. Finally, the total adsorption charge transfer can be obtained as formula: $\Delta Q_t = Q_2 - Q_1$, where Q_2 and Q_1 remark the charge of GaN and C-doped GaN nanosheets after and before adoption of CH₃OH and H₂O molecules. As a matter of fact, negative ΔQ_t indicates that electrons are transferred from adsorbates to the adsorbents of GaN and C-doped GaN nanosheets which act the electron acceptors^[34,35].

The adsorbing of CH₃OH and H₂O molecules on the surfaces of GaN and C-doped GaN nanosheets was defined by the theory “Langmuir” isotherm^[36–39], which indicates the chemisorption between liquids molecules and solid surfaces. The adsorbates of CH₃OH and H₂O molecules are maintained on surfaces of GaN and C-doped GaN with “Langmuir” chemisorption (**Figure 1**).

The changes of charge density analysis in the adsorption process has illustrated that GaN nanosheet shows the Bader charge of -1.382 eV, before adsorption of CH₃OH and H₂O, and -0.595 eV after adsorption of CH₃OH and H₂O, respectively. In addition, C-doped GaN nanosheet shows the Bader charge of -0.656 eV, before adsorption of CH₃OH and H₂O, and -0.360 eV after adsorption of CH₃OH and H₂O, respectively.

Therefore, the changes of charge density for “Langmuir” adsorption of NO, NO₂ and NH₃ on GaN surface alternatively are $\Delta Q_{\text{CH}_3\text{O}@GaN} = +0.787 > \Delta Q_{\text{CH}_3\text{O}@C-GaN} = +0.296$. The values of changes of charge density have shown a more important charge transfer for C-doped GaN nanosheet compared to GaN surface.

To determine the most sensitive structure of GaN and C-doped GaN nanosheets as the selective sensor for detecting CH₃OH_(l), the binding energy of each system has been calculated. Therefore, we have found that the priority for selecting the surface binding of O-atom of CH₃OH_(l) in adsorption site can be impacted by the existence of close atoms in the GaN and C-doped GaN surfaces. The simulated distribution functions of CH₃O@GaN and CH₃O@C–GaN complexes have illustrated that the created clusters lead to the bond lengths of O–Ga in CH₃O–GaN complex is 1.99 \AA and O–C in CH₃O–C–GaN complex is 1.43 \AA (**Figure 1**).

3. Results and discussion

In this verdict, gallium nitride (GaN) and carbon doped gallium nitride (C–GaN) nanosheets have been investigated as the efficient surface because of their structural selectivity for adsorption of CH₃OH towards H₂ production (**Figure 1**). These experiments have been accomplished using spectroscopy analysis through some physical and chemical properties.

3.1. The properties of electronic specification

The electronic structures of CH₃OH in water medium adsorbed on the GaN and C-doped GaN nanosheets have been analyzed to simplify subsequent discussion for interfacial electronic properties using CAM-B3LYP/LANL2DZ, 6-311+G (d,p) basis sets. The graph of partial DOS (PDOS) has illustrated that the p states of the adsorption of (O–) on the GaN (**Figure 2a**) and C-doped GaN (**Figure 2b**) nanosheets are dominant through the conduction band. A distinct metallic feature can be observed in GaN and C-doped GaN nanosheets because of the strong interaction between the p states of C, N, O and the d states of Ga near the Fermi energy. Moreover, the existence of covalent features for these complexes has exhibited the identical energy amount and figure of the PDOS for the p orbitals of C, N, O and d orbitals of Ga (**Figure 2a,b**).

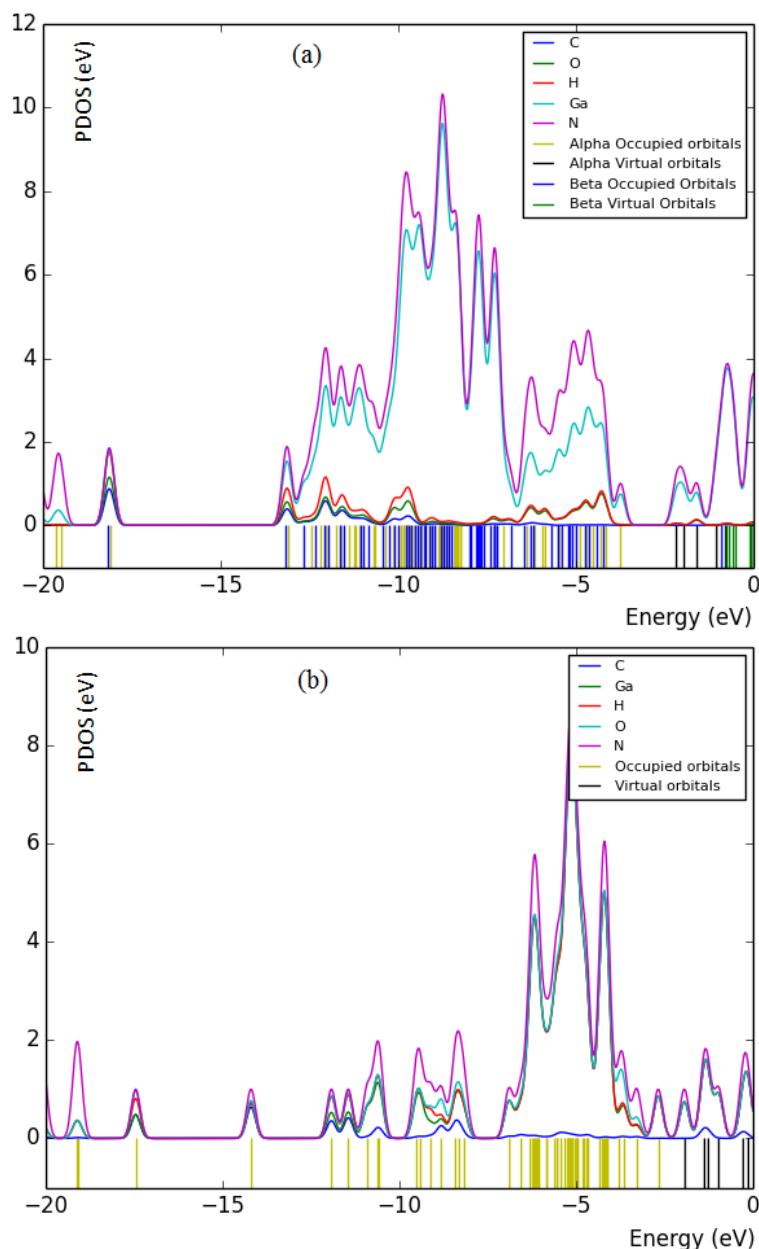


Figure 2. PDOS adsorption of (a) CH₃O@GaN; (b) CH₃O@C-GaN nanosheets with Fermi level = 0.

Figure 2a,b shows that the CH₃OH states in both GaN and C-doped GaN have more contribution at the middle of the conduction band between -5 eV to -10 eV. However, gallium and nitrogen in PDOS of CH₃O@GaN are expanded and close together, but hydrogen, carbon, and oxygen states have minor contributions (**Figure 2a**). Further, not only gallium and nitrogen in PDOS of CH₃O@C-GaN are expanded and close together, but also hydrogen, carbon, and oxygen states exhibit the similar behavior (**Figure 2b**).

The results have been approved by the partial electron density (PDOS) which have showed a certain charge association between GaN & C-doped GaN nanosheets and CH₃OH in water.

In other words, the Ga states in GaN nanosheet have large contributions in the valence band, while C states in C-GaN nanosheet have less contribution. Thus, the above results exhibit that the cluster dominant of non-metallic and metallic features and a certain degree of covalent features can illustrate the increasing of the semiconducting direct band gap of CH₃OH molecules adsorbing on the GaN and C-doped GaN nanosheets.

3.2. Electrostatic properties & “NQR”

In this research, the calculated “nuclear quadrupole resonance” or “NQR” specifications extract form electrostatic properties have been calculated for pyridine and alkyipyridines which is accord to the results of the “nuclear quadrupole moment”, a trait of the nucleus, and the “electric field gradient” or “EFG” in the neighborhood of the nucleus^[40,41].

As the “EFG” at the citation of the nucleus in CH₃OH is allocated by the valence electrons twisted in the particular attachment with close nuclei of GaN and C-doped GaN nanosheets, the “NQR” frequency at which transitions occur is particular for CH₃O@GaN and CH₃O@C–GaN complexes (**Table1**). In “NQR”, nuclei with spin ≥ 1 , there is an electric quadrupole moment which is accompanied with “non-spherical” nuclear charge diffusions. So, the nuclear charge diffusion extracts from that of a sphere as the oblate or prolate form of the nucleus^[40,41].

In this research work, the “electric potential” as the quantity of work energy through carrying over the electric charge from one position to another position in the essence of electric field has been evaluated for CH₃O@GaN and CH₃O@C–GaN complexes using “CAM-B3LYP/EPR-III,LANL2DZ, 6-31+G(d,p)” level of theory (**Table1**).

Table1. The electric potential ($E_p/a.u.$) and Bader charge (Q/e) for elements involving in the adsorption mechanism of CH₃OH on the GaN and C–GaN nanosheets using CAM-B3LYP/EPR-III, 6-311+G (d,p) calculation extracted of “NQR” method.

CH ₃ O@GaN			CH ₃ O@C–GaN		
Atom	Q	E_p	Atom	Q	E_p
C1	-0.138883	-14.492177	C1	-0.14605	-14.512467
O2	-0.24257	-22.027273	O2	-0.17376	-22.045969
Ga3	0.322949	-146.588123	Ga3	0.324268	-146.767356
N4	-0.46868	-18.147423	N4	-0.35983	-18.155333
Ga5	0.306262	-146.612401	Ga5	0.336588	-146.812044
Ga6	0.309491	-146.610467	Ga6	0.333853	-146.812337
N7	-0.35841	-18.152134	N7	-0.35534	-18.166987
Ga8	0.307619	-146.585654	Ga8	0.330507	-146.760619
N9	-0.33082	-18.188336	N9	-0.35918	-18.207219
N10	-0.45791	-18.14294	N10	-0.34344	-18.151422
Ga11	0.304534	-146.62799	C11	0.149105	-14.558703
Ga12	0.322382	-146.594445	Ga12	0.341117	-146.766486
N13	-0.46026	-18.142017	N13	-0.35558	-18.154238
Ga14	0.317285	-146.555721	Ga14	0.345001	-146.760011
N15	-0.32395	-18.181239	N15	-0.35379	-18.202835
H16	0.087583	-1.117471	H16	0.082743	-1.130149
H17	0.059464	-1.102232	H17	0.067091	-1.117932
H18	0.077249	-1.118892	H18	0.07037	-1.14026
H19	0.076651	-1.070412	H19	0.066315	-1.094491

As the electric potential for a system of point charges is similar to the amount of the point charges’ individual potentials, the computations are carried out easily on the basis of the total of potential fields which are scalar in lieu of total of the electric fields which are vector and much more tough than the potential field parameter^[42–45].

Furthermore, in **Figure 3a,b**, it has been sketched the “electric potential” of nuclear quadrupole resonance for some atoms of hydrogen, carbon, nitrogen, oxygen, and gallium in the adsorption process of CH₃OH on the GaN (**Figure 3a**), and C–GaN nanosheets (**Figure 3b**) which have been calculated by “CAM-B3LYP/EPR-III, 6-311+G (d,p), LANL2DZ”.

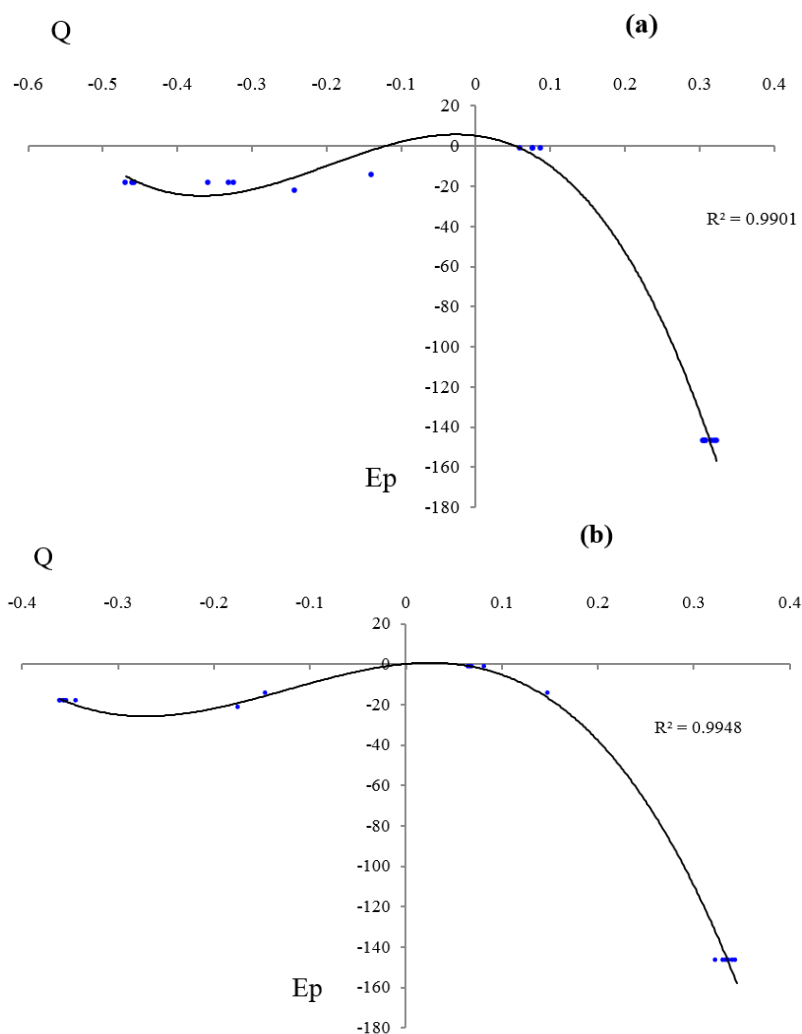


Figure 3. The electric potential versus Bader charge through NQR calculation for adsorption clusters of (a) CH₃O@GaN; (b) CH₃O@C–GaN using CAM-B3.LYP/EPR-III, LANL2.DZ, 6-31+G(d,p).

In **Figure 3a**, it has been described the plot of electric potential for Bader charge of different atoms while CH₃OH adsorbs on the GaN surface, while **Figure 3b** shows the influence of the replacement of gallium metal element in “GaN” surface with “C”. It’s vivid that the curve of “GaN” is waved by the carbon element (**Figure 3b**). The plot for electric potential versus atomic charge has been shown around carbon doping of the GaN which presents the electron accepting characteristics of this element via the electron donor of oxygen atom in CH₃OH with $R^2 = 0.9948$ (**Figure 3b**).

The amounts of changes of charge density have exhibited a more important charge transfer from O atom of CH₃O⁻ anion of CH₃OH as the electron donor adsorbed onto GaN and C-doped GaN nanosheets which play a role as the electron acceptors due to the production of the covalent bond of “O–Ga” and “O–C–GaN”.

In fact, Ga and C sites in GaN and C-doped gallium nitride, respectively, have more interaction energy from “Van der Waals’ forces” with CH₃OH molecules that can cause more stability towards coating specifications on the surface. It has been estimated that the precedence for picking out the crystal binding of “O-atom” in CH₃O⁻ anion in adsorption position can be impressed by the essence of neighboring elements of

gallium and nitrogen in the GaN and C-doped GaN (**Figure 3a,b**).

3.3. Magnetism and atomic charge analysis

Nuclear magnetic resonance spectrums of CH₃O@GaN and CH₃O@C–GaN complexes approve potent sensor of gallium nitride and carbon doping of gallium nitride for adsorbing the methanol in water and running the production of hydrogen. GaN and C–GaN surfaces can unravel the formation of the covalent binding between CH₃OH (adsorbate) and surface (adsorbent).

From the “DFT” calculations, it has been attained the “chemical shielding” «CS» tensors in the principal axes system to estimate the “isotropic chemical-shielding” «CSI» and “anisotropic chemical-shielding” «CSA»^[46–50]:

$$\sigma_{iso} = (\sigma_{11} + \sigma_{22} + \sigma_{33})/3 \quad (1)$$

$$\sigma_{aniso} = \sigma_{33} - (\sigma_{22} + \sigma_{11})/2 \quad (2)$$

The chemical shielding extracts from “Nuclear magnetic resonance” or “NMR” can be applied for allocating the structural and geometrical specifications of materials. As a matter of fact, “Gauge Invariant Atomic Orbital” or “GIAO” methodology has been recommended as a valid methodology for “NMR” parameter computations^[51–58].

The “NMR” data of isotropic “ σ_{iso} ” and anisotropic shielding tensor “ σ_{aniso} ” of atoms including H, C, N, O and Ga through interaction of CH₃OH with GaN/C–GaN surfaces towards formation of CH₃O@GaN, CH₃O@C–GaN complexes and hydrogen gas have been computed by “Gaussian 16 revision C.01” program package^[31] and been shown in **Table 2**.

Table 2. NMR properties of chemical shielding tensors (σ_{iso} & σ_{aniso} /ppm) of H, C, N, O and Ga in the attachment of CH₃OH with GaN/C–GaN surfaces through formation of CH₃O@GaN, CH₃O@C–GaN complexes.

CH ₃ O@GaN			CH ₃ O@C–GaN		
Atom	σ_{iso}	σ_{aniso}	Atom	σ_{iso}	σ_{aniso}
C1	179.2159	36.9065	C1	154.6499	27.4129
O2	150.9691	2974.7309	O2	354.8987	1124.8774
Ga3	18,758.6499	30,577.9370	Ga3	19,183.9008	94,666.3864
N4	216.2120	669.9269	N4	1596.0584	2360.8485
Ga5	18,455.2566	31,327.7419	Ga5	31,627.2684	168,594.4964
Ga6	18,149.2904	32,713.7441	Ga6	33,369.2782	171,759.8387
N7	90.9294	464.4114	N7	1549.1214	3515.8318
Ga8	18,485.2174	30,431.4337	Ga8	16,340.7312	92,617.2317
N9	218.9173	642.6002	N9	3425.9587	8314.4536
N10	284.5798	874.2235	N10	3839.2101	5176.1081
Ga11	2914.3282	61,977.2718	C11	657.4748	456.9113
Ga12	18,698.0002	31,192.1416	Ga12	28,908.1246	103,351.9912
N13	211.0279	717.2403	N13	1525.2165	2431.6412
Ga14	9260.9374	74,714.9298	Ga14	16,656.4595	64,475.8664
N15	501.4350	774.0516	N15	2737.5337	7019.4326
H16	29.5211	7.4972	H16	16.5222	8.7048
H17	27.8756	35.8204	H17	6.7072	56.5045
H18	32.4537	18.8661	H18	2.9067	21.0737
H19	38.4521	31.7367	H19	15.5484	121.4571

In **Table 2**, “NMR” data has reported the notable amounts for C atom which has been doped on the GaN surface through CH₃OH adsorption surrounded with H₂O molecules and H₂ & CO₂ productions. In fact, the adsorption of CH₃OH introduces spin polarization on the C-doped GaN nanosheet surface which indicates that this surface might be applied as magnetic methanol detector (**Figure 4**).

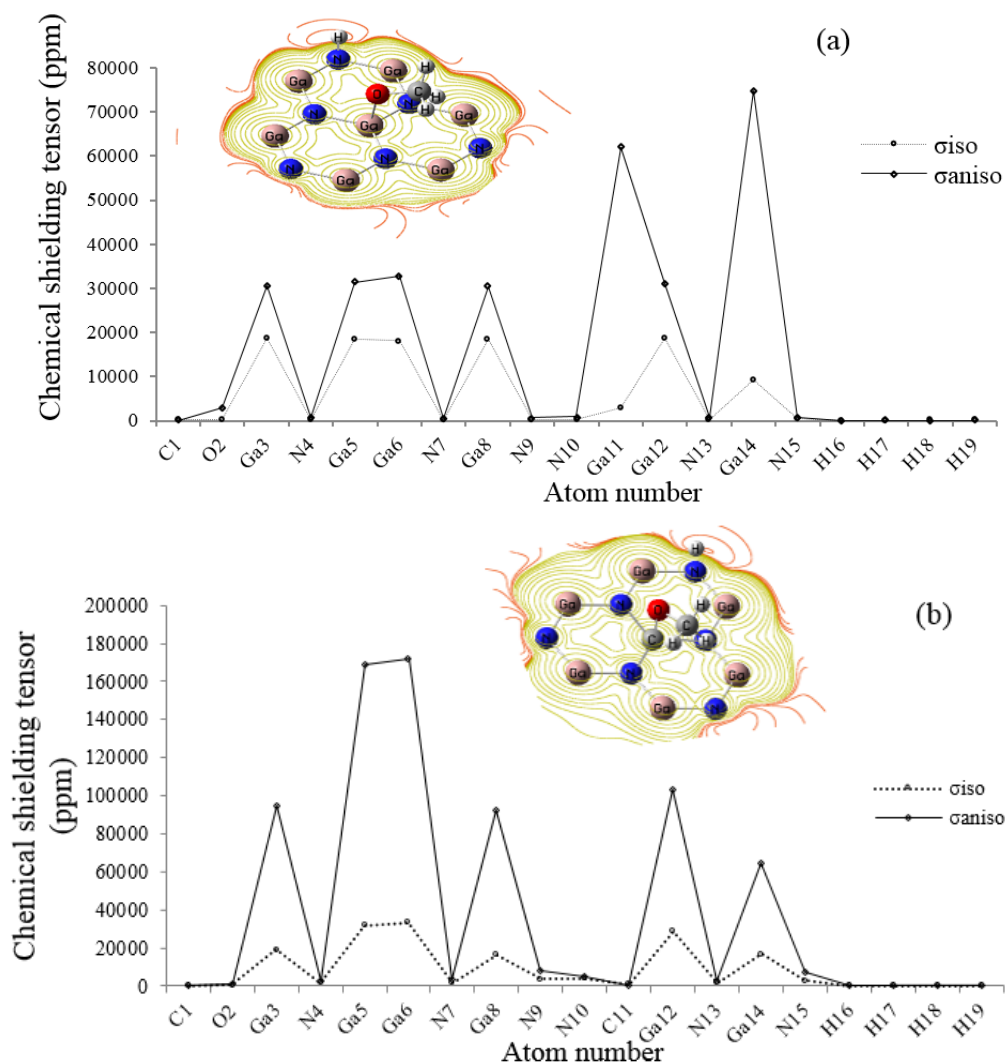


Figure 4. Chemical shielding tensors of σ_{iso} and σ_{aniso} extracts from “NMR” spectroscopy for CH₃OH adsorption on the (a) GaN; (b) C-doped GaN nanosheets towards production of hydrogen gas.

It is revealed that the “isotropic” and “anisotropy” shielding tensors augment with the negative Bader charge (**Table 1**) in methanol penetrated by “O-atom” in the CH₃O–GN complex. It has been exhibited that the shielding tensor graph of “O-atom” has the same tendency, however a considerable deviation from gallium element (**Figure 4a,b**).

In **Figure 4a,b**, the maximum fluctuation of “isotropic” and “anisotropy” shielding tensors for Ga11, Ga12, Ga14 in CH₃O@GaN cluster has been observed (**Figure 4a**), while the maximum fluctuation of “isotropic” and “anisotropy” shielding tensors for Ga3, Ga5, Ga6 in CH₃O@C–GaN cluster has been seen (**Figure 4b**).

3.4. “IR” insight & thermodynamic analysis

The “IR” spectrums for adsorption of CH₃OH_(l) on the surfaces of GaN and C–GaN towards the formation of CH₃O@GaN and CH₃O@C–GaN complexes, respectively, have been reported in **Figure 5a,b**.

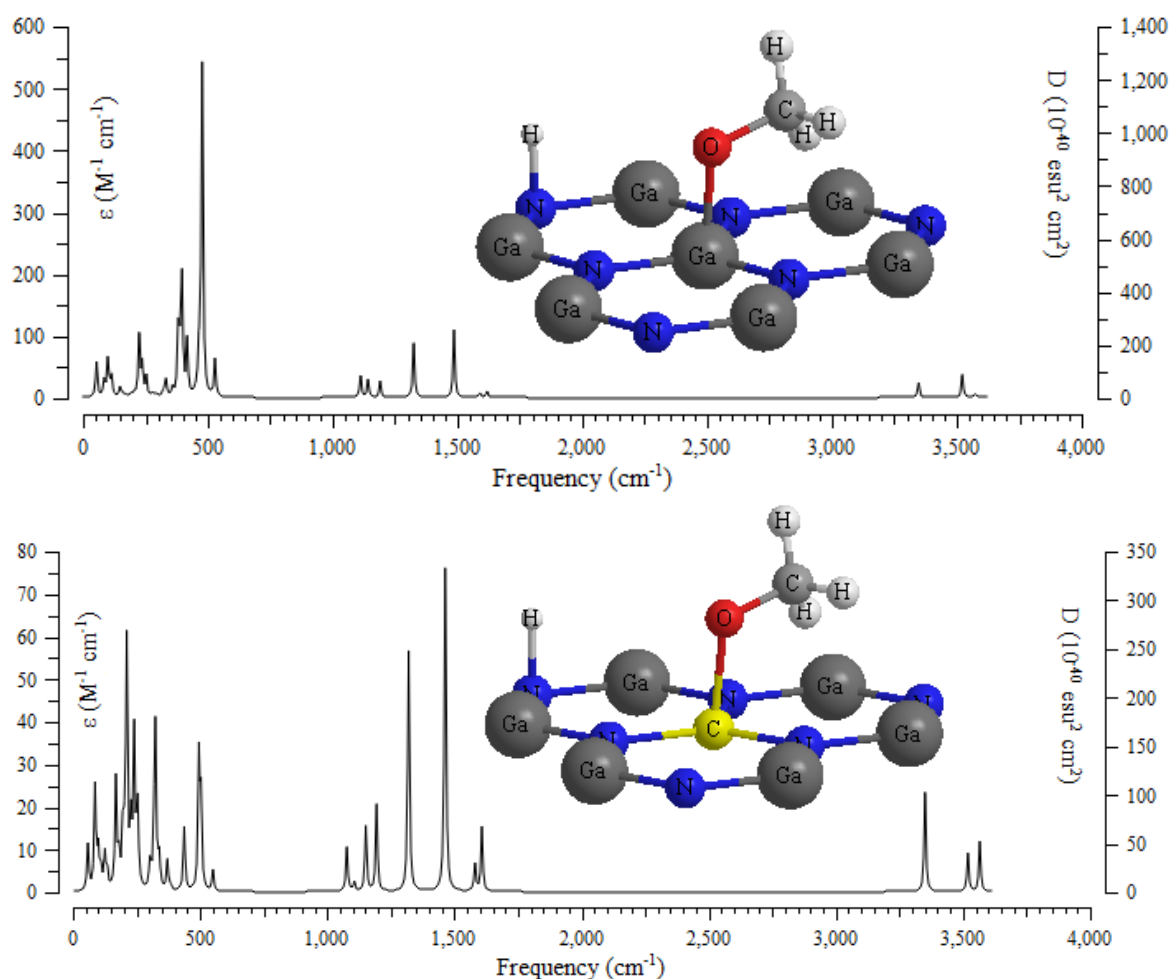


Figure 5. The Frequency (cm^{-1}) changes through the “IR” spectrums for (a) $\text{CH}_3\text{O@GaN}$; (b) $\text{CH}_3\text{O@C-GaN}$ complexes.

The graphs of **Figure 5a,b** has been observed in the frequency range between 50 cm^{-1} – 3500 cm^{-1} for the complexes of $\text{CH}_3\text{O@GaN}$ and $\text{CH}_3\text{O@C-GaN}$, respectively, with a sharp peak around 1500 cm^{-1} for both $\text{CH}_3\text{O@GaN}$ and $\text{CH}_3\text{O@C-GaN}$ complexes (**Figure 5a,b**).

In this part, the stability of complexes including methanol adsorption on graphitic gallium nitride (GaN) and carbon doping of gallium nitride (C-GaN) has been investigated through thermodynamic properties which define the reaction of methanol in water towards production of hydrogen and carbon dioxide in the gas phase that are trapped in the gallium and carbon coordination sphere (**Table 3**).

Table 3. The thermodynamic properties of $\text{CH}_3\text{OH}_{(l)}$ and $\text{H}_2\text{O}_{(l)}$ adsorbed on the surfaces of GaN and C-GaN towards the formation of $\text{CH}_3\text{O@GaN}$ & $\text{CH}_3\text{O@C-GaN}$ complexes and the products of $\text{H}_{2(g)}$ & $\text{CO}_{2(g)}$.

Compound	$\Delta E^0 \times 10^{-4}$ (kcal/mol)	$\Delta H^0 \times 10^{-4}$ (kcal/mol)	$\Delta G^0 \times 10^{-4}$ (kcal/mol)	S^0 (Cal/K.mol)	Dipole moment (Debye)
$\text{CH}_3\text{OH}_{(l)}$	-7.1568	-7.1568	-7.1584	55.576	1.3748
$\text{H}_2\text{O}_{(l)}$	-4.7211	-4.7211	-4.7224	44.777	1.5981
$\text{H}_{2(g)}$	-0.0714	-0.0714	-0.0723	30.851	0.0000
$\text{CO}_{2(g)}$	-11.6656	-11.6655	-1.6671	52.674	0.0000
GaN	-21.4958	-21.4957	-21.4998	137.460	0.6307
C-GaN	-744.0161	-744.0160	-744.0199	130.698	1.9560
$\text{CH}_3\text{O@GaN}$	-863.0549	-863.0549	-863.0593	150.485	0.6776
$\text{CH}_3\text{O@C-GaN}$	-746.0152	-746.0151	-746.0192	134.809	0.2953

Concerning adsorption process, the thermodynamic properties were evaluated for initial compounds of $\text{CH}_3\text{OH}_{(l)}$ and $\text{H}_2\text{O}_{(l)}$ adsorbed on the surfaces of GaN and C–GaN towards the formation of $\text{CH}_3\text{O@GaN}$ & $\text{CH}_3\text{O@C–GaN}$ complexes and finally the products of $\text{H}_{2(g)}$ and $\text{CO}_{2(g)}$ (**Table 3**).

In addition, the high amounts of the “Langmuir” adsorption isotherm graphs based on gibbs free energy ($\Delta G^\circ_{\text{ads}}$) has been evaluated for interactions between $\text{CH}_3\text{OH}_{(l)}$ molecules on the surfaces of GaN and C–GaN nanosheets with $R^2 = 0.9999$ (**Figure 6**). The order of $\Delta G^\circ_{\text{ads}}$ for $\text{CH}_3\text{OH}_{(l)}$ molecules adsorption on GaN nanosheet has indicated more stability compared to Gibbs free energy of $\text{CH}_3\text{OH}_{(l)}$ molecules adsorption on C–GaN nanosheet (**Figure 6**).

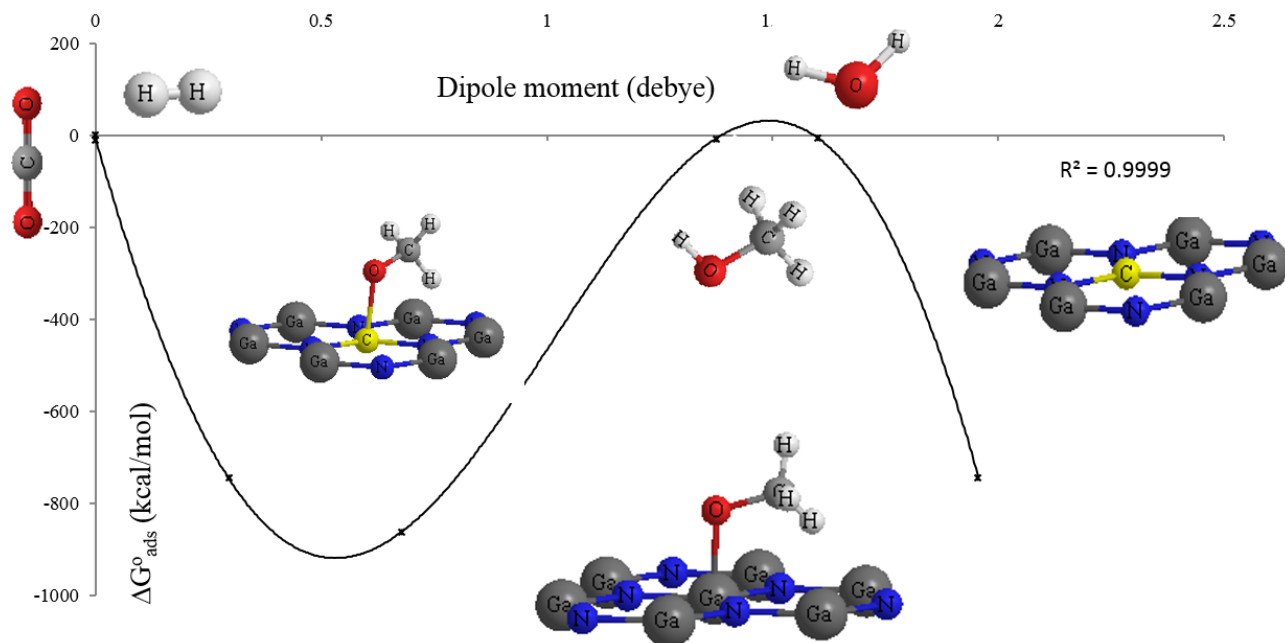


Figure 6. The alterations of Gibbs free energy ($\Delta G^\circ_{\text{ads}}$) for $\text{CH}_3\text{OH}_{(l)}$ and $\text{H}_2\text{O}_{(l)}$ adsorbed on the surfaces of GaN and C–GaN towards the formation of $\text{CH}_3\text{O@GaN}$ & $\text{CH}_3\text{O@C–GaN}$ complexes and the products of $\text{H}_{2(g)}$ & $\text{CO}_{2(g)}$.

The adsorptive capacity of $\text{CH}_3\text{OH}_{(l)}$ and $\text{H}_2\text{O}_{(l)}$ adsorbed on the surfaces of GaN and C–GaN is approved by the relative energy ($\Delta E^\circ_{\text{ads}}$) amounts as formula:

$$\Delta E^\circ_{\text{ads}} = \Delta E^\circ_{\text{CH}_3\text{O@GaN}} - (\Delta E^\circ_{\text{CH}_3\text{OH}_{(l)}} + \Delta E^\circ_{\text{GaN}}) \quad (3)$$

$$\Delta E^\circ_{\text{ads}} = \Delta E^\circ_{\text{CH}_3\text{O@C–GaN}} - (\Delta E^\circ_{\text{CH}_3\text{OH}_{(l)}} + \Delta E^\circ_{\text{C–GaN}}) \quad (4)$$

Table 3 has shown that the adsorbing of $\text{CH}_3\text{OH}_{(l)}$ on the surfaces of GaN and C–GaN nanosheets must have both “physical” and “chemical” nature. All the measured relative adsorption energies ($\Delta E^\circ_{\text{ads}}$) are almost identical, and exhibit the accord of the estimated data by all methods and the accuracy of the calculations (**Figure 6**). In fact, Ga sites in GaN and C sites in C–GaN nanosheets have higher interaction energy from Van der Waals’ forces with gas molecules including $\text{CH}_3\text{OH}_{(l)}$ molecules that can make them highly stable.

Furthermore, the results of **Table 3** has indicated that $\text{CH}_3\text{O@GaN}$ & $\text{CH}_3\text{O@C–GaN}$ nanosheets have the largest gap of Gibbs free energy adsorption which defines the changes between Gibbs free energy of initial compounds ($\Delta G^\circ_{\text{CH}_3\text{OH}_{(l)}}$, $\Delta G^\circ_{\text{H}_2\text{O}}$) and product compounds ($\Delta G^\circ_{\text{H}_{2(g)}}$, $\Delta G^\circ_{\text{CO}_{2(g)}}$) through polarizability on the GaN and C–GaN nanosheets (**Figure 6**). However, GaN and C–GaN nanosheets seem to possess enough efficiency for adsorption $\text{CH}_3\text{OH}_{(l)}$ molecules through charge transfer from oxygen to the gallium and carbon elements due to intra-atomic and interatomic interactions.

In a recent work, WANG and co-workers have provided a systematic explanation of the adsorption between the hydroxyl groups and the GaN surface. DFT calculations and X-ray photoelectron spectroscopy

(XPS) were carried out to investigate the hydroxyl groups on a GaN surface^[59]. It was indicated that adsorption of hydroxyl groups is more favorable near the center location than near gallium atoms. In fact, surface treatments of GaN with piranha and HCl-based solutions were studied via XPS, and peak shifts in the “Ga” 2p and “O” 1s XPS spectra were caused by the signal change resulting from surface hydroxyl groups^[59]. Moreover, the thermodynamic results showed that the high hydroxyl group coverage is more likely to be present on the GaN surface which has a good accord with our results.

Some studies have indicated that the exposed m-plane of GaN exhibited particularly high activity toward methane C–H bond activation and the quantum efficiency increased linearly as a function of light intensity. The incorporation of a Si-donor or Mg-acceptor dopants into GaN also has a large influence on the photocatalytic performance^[60].

By comparing the activation barrier of the rate-limiting step on both surfaces, the results showed that the C–H bond cleavage of the CH₃ species have the highest activation barrier for both catalysts^[61].

4. Conclusion

The current research wanted to remark the illustration of CH₃OH in water adsorbed on GaN and C-doped GaN nanosheets which catalyze the H₂ producing. Particularly, the structural, energetic, and infrared adsorption properties of linearly “atop” for CH₃OH_(l) molecules adsorbing on GaN and C-doped GaN surfaces have been explored by using DFT calculations.

The values of changes of charge density have shown a more important charge transfer for C-doped GaN compared to GaN which act both as the electron acceptor through the reaction of methanol and water as initial compounds.

In fact, Ga sites in GaN and C sites in C-doped GaN nanosheets have high interaction energy from Van der Waals’ forces with CH₃OH and H₂O that can make them highly stable. Finally, our molecular simulation consequences have exhibited the existence of the gibbs free energy of CH₃OH_(l) and H₂O_(l) adsorbed on the surfaces of GaN and C–GaN that approves the recovery of adsorption susceptibility of GaN and C-doped GaN surfaces. These findings may open up a various catalytic path for the directly efficient usage of CH₃OH.

Author contributions

Conceptualization and idea, FM; methodology, FM and MM; software, FM and MM; validation, FM; formal analysis, FM and MM; resources, MM; investigation, FM and MM; data curation, FM and MM; writing—original draft preparation, FM; writing—review and editing, MM; visualization, FM and MM; supervision FM; project administration, FM. All authors have read and agreed to the published version of the manuscript.

Acknowledgments

In successfully completing this paper and its research, the authors are grateful to Kastamonu University for their support through the office, library, and scientific websites.

Conflict of interest

The authors declare no conflict of interest.

References

1. Ikawa Y, Lee K, Ao JP, Ohno Y. Two-dimensional device simulation of AlGaIn/GaN heterojunction FET side-gating effect. *Japanese Journal of Applied Physics* 2014; 53: 114302. doi: 10.7567/JJAP.53.114302
2. Podolska A, Seeber RM, Mishra UK, et al. Detection of biological reactions by AlGaIn/GaN biosensor. In:

- Proceedings of COMMAD 2012; 12–14 December 2012; Melbourne, VIC, Australia. pp. 75–76.
3. Mollaamin F, Monajjemi M. Graphene-based resistant sensor decorated with Mn, Co, Cu for nitric oxide detection: Langmuir adsorption & DFT method. *Sensor Review* 2023; 43(4): 266–279. doi:10.1108/SR-03-2023-0040
 4. Pearton SJ, Kang BS, Kim SK, et al. GaN-based diodes and transistors for chemical, gas, biological and pressure sensing. *Journal of Physics: Condensed Matter* 2004; 16: R961–R994. doi: 10.1088/0953-8984/16/29/R02
 5. Mollaamin F, Monajjemi M, Salemi S, Baei MT. A dielectric effect on normal mode analysis and symmetry of BNNT nanotube. *Fullerenes, Nanotubes and Carbon Nanostructures* 2011; 19(3): 182–196, doi: 10.1080/15363831003782932
 6. Monajjemi M, Mahdavian L, Mollaamin F, Khaleghian M. Interaction of Na, Mg, Al, Si with carbon nanotube (CNT): NMR and IR study. *Russian Journal of Inorganic Chemistry* 2009; 54: 1465–1473. doi: 10.1134/S0036023609090216
 7. Mollaamin F, Monajjemi M. Harmonic linear combination and normal mode analysis of semiconductor nanotubes vibrations. *Journal of Computational and Theoretical Nanoscience* 2015; 12(6): 1030–1039. doi: 10.1166/jctn.2015.3846
 8. Yong Y, Jiang H, Li X, et al. The cluster-assembled nanowires based on $M_{12}N_{12}$ ($M = Al$ and Ga) clusters as potential gas sensors for CO, NO, and NO_2 detection. *Physical Chemistry Chemical Physics* 2016; 18(31): 21431–21441. doi: 10.1039/C6CP02931K
 9. Monajjemi M, Farahani N, Mollaamin F. Thermodynamic study of solvent effects on nanostructures: Phosphatidylserine and phosphatidylinositol membranes. *Physics and Chemistry of Liquids* 2012; 50: 161–172. doi: 10.1080/00319104.2010.527842
 10. Mollaamin F, Monajjemi M. Tribocorrosion framework of (Iron, Nickel, Zinc)-doped graphene nanosheet: New sights into sulfur dioxide and hydrogen sulfide removal using DFT/TD-DFT methods. *Journal of Bio- and Tribo-Corrosion* 2023; 9: 47. doi: 10.1007/s40735-023-00768-3
 11. Monajjemi M, Najafpour J, Mollaamin F. $(3,3)_4$ Armchair carbon nanotube in connection with PNP and NPN junctions: Ab Initio and DFT-based studies. *Fullerenes Nanotubes and Carbon Nanostructures* 2013; 21(3): 213–232. doi: 10.1080/1536383X.2011.597010
 12. Monajjemi M, Baheri H, Mollaamin F. A percolation model for carbon nanotube-polymer composites using the Mandelbrot-Given curve. *Journal of Structural Chemistry* 2011; 52: 54–59. doi: 10.1134/S0022476611010070
 13. Mollaamin F, Monajjemi M. Hexagonal honeycomb PL-GaN nanosheet as adsorbent surface for gas molecules sensing: A quantum chemical study. *Surface Review and Letters* 2023. doi: 10.1142/S0218625X24500057
 14. Kente T, Mhlanga SD. Gallium nitride nanostructures: Synthesis, characterization and applications. *Journal of Crystal Growth* 2016; 444: 55–72. doi: 10.1016/j.jcrysgro.2016.03.033
 15. Yong Y, Cui H, Zhou Q, et al. Adsorption of gas molecules on a graphitic GaN sheet and its implications for molecule sensors. *RSC Advances* 2017; 7(80): 51027–51035. doi: 10.1039/c7ra11106a
 16. Khan AH, Rao MV. Gallium nitride (GaN) nanostructures and their gas sensing properties: A review. *Sensors* 2020; 20(13): 3889. doi: 10.3390/s20143889.
 17. Park K, Lee J, Kim D, et al. Synthesis of polytypic gallium phosphide and gallium arsenide nanowires and their application as photodetectors. *ACS Omega* 2019; 4(2): 3098–3104. doi: 10.1021/acsomega.8b03548
 18. Šetka M, Claros M, Chmela O, Vallejos S. Photoactivated materials and sensors for NO_2 monitoring. *Journal of Materials Chemistry C* 2021; 9(47): 16804–16827. doi: 10.1039/D1TC04247E
 19. Geng X, Liu X, Mawella-Vithanage L, et al. Photoexcited NO_2 enables accelerated response and recovery kinetics in light-activated NO_2 gas sensing. *ACS Sensors* 2021; 6: 4389–4397. doi: 10.1021/acssensors.1c01694
 20. Shin J, Han S, Noh S, et al. Room-temperature operation of light-assisted NO_2 gas sensor based on GaN nanowires and graphene. *Nanotechnology* 2021; 32: 505201. doi: 10.1088/1361-6528/ac2427
 21. Pinder RW, Walker JT, Bash JO, et al. Quantifying spatial and temporal variability in atmospheric ammonia with in situ and space-based observations. *Geophysical Research Letters* 2011; 38: L04802. doi: 10.1029/2010GL046146
 22. Langridge JM, Lack D, Brock CA, et al. Evolution of aerosol properties impacting visibility and direct climate forcing in an ammonia-rich urban environment. *Journal of Geophysical Research: Atmospheres* 2012; 117(D21): D00v11. doi: 10.1029/2011jd017116
 23. Lamarque JF, Kyle GP, Meinshausen M, et al. Global and regional evolution of short-lived radiatively-active gases and aerosols in the representative concentration pathways. *Climatic Change* 2011; 109: 191–212. doi: 10.1007/s10584-011-0155-0
 24. Liu C, Kang J, Huang ZQ, et al. Gallium nitride catalyzed the direct hydrogenation of carbon dioxide to dimethyl ether as primary product. *Nature Communications* 2021; 12: 2305. doi: 10.1038/s41467-021-22568-4
 25. Zhou W, Cheng K, Kang J, et al. New horizon in C1 chemistry: Breaking the selectivity limitation in transformation of syngas and hydrogenation of CO_2 into hydrocarbon chemicals and fuels. *Chemical Society Reviews* 2019; 48: 3193–3228. doi: 10.1039/C8CS00502H
 26. Leonzio G. State of art and perspectives about the production of methanol, dimethyl ether and syngas by carbon dioxide hydrogenation. *Journal of CO_2 Utilization* 2018; 27: 326–354. doi: 10.1016/j.jcou.2018.08.005

27. Mollaamin F, Monajjemi M. In silico-DFT investigation of nanocluster alloys of Al-(Mg, Ge, Sn) coated by nitrogen heterocyclic carbenes as corrosion inhibitors. *Journal of Cluster Science* 2023; 1–18. doi: 10.1007/s10876-023-02436-5
28. Mollaamin F, Monajjemi M. Molecular modelling framework of metal-organic clusters for conserving surfaces: Langmuir sorption through the TD-DFT/ONIOM approach. *Molecular Simulation* 2023; 49(4): 365–376. doi: 10.1080/08927022.2022.2159996
29. Singh AK, Zhuang HL, Hennig RG. Ab initio synthesis of single-layer III-V materials. *Physical Review B (PRB)* 2014; 89: 245431. doi: 10.1103/PhysRevB.89.245431
30. Dennington R, Keith TA, Millam JM. *GaussView, Version 6*. Semichem Inc.; 2016.
31. Frisch MJ, Trucks GW, Schlegel HB, et al. *Gaussian 16, Revision C.01*. Gaussian, Inc.; 2016.
32. Perdew JP, Burke K, Ernzerhof M. Generalized gradient approximation made simple. *Physical Review Letters* 1996; 77: 3865. doi: 10.1103/PhysRevLett.77.3865
33. Henkelman G, Arnaldsson A, Jónsson H. A fast and robust algorithm for Bader decomposition of charge density. *Computational Materials Science* 2006; 36(3): 354–360. doi: 10.1016/j.commatsci.2005.04.010
34. Mollaamin F, Monajjemi M. Electric and magnetic evaluation of aluminum-magnesium nanoalloy decorated with germanium through heterocyclic carbenes adsorption: A density functional theory study. *Russian Journal of Physical Chemistry B* 2023; 17(3): 658–672. doi: 10.1134/S1990793123030223
35. Mao Y, Yuan J, Zhong J. Density functional calculation of transition metal adatom adsorption on graphene. *Journal of Physics: Condensed Matter* 2008; 20(11): 115209.
36. Mollaamin F, Monajjemi M. Corrosion inhibiting by some organic heterocyclic inhibitors through Langmuir adsorption mechanism on the Al-X (X = Mg/Ga/Si) alloy surface: A study of quantum three-layer method of CAM-DFT/ONIOM. *Journal of Bio- and Tribo-Corrosion* 2023; 9: 33. doi: 10.1007/s40735-023-00751-y
37. Mollaamin F, Shahriari S, Monajjemi M, Khalaj Z. Nanocluster of aluminum lattice via organic inhibitors coating: A study of freundlich adsorption. *Journal of Cluster Science* 2023; 34: 1547–1562. doi: 10.1007/s10876-022-02335-1
38. Monajjemi M, Noei M, Mollaamin F. Design of fMet-tRNA and calculation of its bonding properties by quantum mechanics. *Nucleosides, Nucleotides & Nucleic Acids* 2010; 29(9): 676–683. doi: 10.1080/15257771003781642
39. Monajjemi M, Mollaamin F, Gholami MR, et al. Quantum chemical parameters of some organic corrosion inhibitors, pyridine, 2-picoline 4-picoline and 2,4-lutidine, adsorption at aluminum surface in hydrochloric and nitric acids and comparison between two acidic media. *Main Group Metal Chemistry* 2003; 26: 349–362. doi: 10.1515/MGMC.2003.26.6.349
40. Mollaamin F, Monajjemi M. Tailoring and functionalizing the graphitic-like GaN and GaP nanostructures as selective sensors for NO, NO₂, and NH₃ adsorbing: A DFT study. *Journal of Molecular Modeling* 2023; 29: 170. doi: 10.1007/s00894-023-05567-8
41. Shahriari S, Mollaamin F, Monajjemi M. Increasing the performance of {[1-x-y] LiCo_{0.3}Cu_{0.7}] (Al and Mg doped) O₂}, xLi₂MnO₃, yLiCoO₂ composites as cathode material in lithium-ion battery: Synthesis and characterization. *Micromachines* 2023; 14: 241. doi: 10.3390/mi14020241
42. Mollaamin F, Monajjemi M. Transition metal (X = Mn, Fe, Co, Ni, Cu, Zn)-doped graphene as gas sensor for CO₂ and NO₂ detection: A molecular modeling framework by DFT perspective. *Journal of Molecular Modeling* 2023; 29: 119. doi: 10.1007/s00894-023-05526-3
43. Garroway AN. Appendix K: Nuclear quadrupole resonance. In: Gibson JMD, Lockwood JR. *Alternatives for Landmine Detection*. Rand Corporation; 2003.
44. Mollaamin F. Computational methods in the drug delivery of carbon nanocarriers onto several compounds in sarraceniaceae medicinal plant as monkeypox therapy. *Computation* 2023; 11(4): 84. doi: 10.3390/computation11040084
45. Young HD, Freedman RA, Ford AL. *Sears and Zemansky's University Physics with Modern Physics*, 13th ed. Addison-Wesley; 2012. p. 754.
46. Mollaamin F, Monajjemi M. Doping of graphene nanostructure with iron, nickel and zinc as selective detector for the toxic gas removal: A density functional theory study. *C* 2023; 9(1): 20. doi: 10.3390/c9010020
47. Zadeh MAA, Lari H, Kharghanian L, et al. Density functional theory study and anti-cancer properties of shyshaq plant: In view point of nano biotechnology. *Journal of Computational and Theoretical Nanoscience* 2015; 12: 4358–4367. doi: 10.1166/jctn.2015.4366
48. Mollaamin F, Monajjemi M. Graphene embedded with transition metals for capturing carbon dioxide: Gas detection study using QM methods. *Clean Technologies* 2023; 5: 403–417. doi: 10.3390/cleantechnol5010020
49. Ghalandari B, Monajjemi M, Mollaamin F. Theoretical investigation of carbon nanotube binding to dna in view of drug delivery. *Journal of Computational and Theoretical Nanoscience* 2011; 8: 1212–1219. doi: 10.1166/jctn.2011.1801
50. Bakhshi K, Mollaamin F, Monajjemi M. Exchange and correlation effect of hydrogen chemisorption on nano V(100) surface: A DFT study by generalized gradient approximation (GGA). *Journal of Computational and Theoretical Nanoscience* 2011; 8: 763–768. doi: 10.1166/jctn.2011.1750

51. Monajjemi M, Khaleghian M, Tadayonpour N, Mollaamin F. The effect of different solvents and temperatures on stability of single-walled carbon nanotube: A QM/MD study. *International Journal of Nanoscience* 2010; 9(5): 517–529. doi: 10.1142/S0219581X10007071
52. Khalili Hadad B, Mollaamin F, Monajjemi M. Biophysical chemistry of macrocycles for drug delivery: A theoretical study. *Russian Chemical Bulletin* 2011; 60: 238–241. doi: 10.1007/s11172-011-0039-5
53. Mollaamin F, Ilkhani A, Sakhaei N, et al. Thermodynamic and solvent effect on dynamic structures of nano bilayer-cell membrane: Hydrogen bonding study. *Journal of Computational and Theoretical Nanoscience* 2015; 12: 3148–3154. doi: 10.1166/jctn.2015.4092
54. Tahan A, Mollaamin F, Monajjemi M. Thermochemistry and NBO analysis of peptide bond: Investigation of basis sets and binding energy. *Russian Journal of Physical Chemistry A* 2009; 83: 587–597. doi: 10.1134/S003602440904013X
55. Khaleghian M, Zahmatkesh M, Mollaamin F, Monajjemi M. Investigation of solvent effects on armchair single-walled carbon nanotubes: A QM/MD study. *Fullerenes, Nanotubes and Carbon Nanostructures* 2011; 19: 251–261. doi: 10.1080/15363831003721757
56. Monajjemi M, Mollaamin F, Shojaei S. An overview on coronaviruses family from past to COVID-19: Introduce some inhibitors as antiviruses from Gillan's plants. *Biointerface Research in Applied Chemistry* 2020; 3: 5575–5585. doi: 10.33263/BRIAC103.575585
57. Sarasia EM, Afsharnezhad S, Honarparvar B, et al. Theoretical study of solvent effect on NMR shielding tensors of luciferin derivatives. *Physics and Chemistry of Liquids* 2011; 49: 561–571. doi: 10.1080/00319101003698992
58. Monajjemi M, Baie MT, Mollaamin F. Interaction between threonine and cadmium cation in $[\text{Cd}(\text{Thr})_n]^{2+}$ ($n = 1-3$) complexes: Density functional calculations. *Bulletin of the Academy of Sciences of the USSR Division of Chemical Science* 2010; 59: 886–889. doi: 10.1007/s11172-010-0181-5
59. Wang H, Zhang H, Liu J, et al. Hydroxyl group adsorption on GaN (0001) surface: First principles and XPS studies. *Journal of Electronic Materials* 2019; 48(4): 2430–2437. doi: 10.1007/s11664-019-07011-1
60. Li L, Fan S, Mu X, et al. Photoinduced conversion of methane into benzene over GaN nanowires. *Journal of the American Chemical Society* 2014; 136(22): 7793–7796. doi: 10.1021/ja5004119
61. Mollaamin F, Monajjemi M. Application of DFT and TD-DFT on Langmuir adsorption of nitrogen and sulfur heterocycle dopants on an aluminum surface decorated with magnesium and silicon. *Computation* 2023; 11: 108. doi: 10.3390/computation11060108